

---

# On Delay-Based Linear Models and Robust Control of Cavity Flows

Xin Yuan<sup>1</sup>, Mehmet Önder Efe<sup>2</sup>, and Hitay Özbay<sup>3</sup>

<sup>1</sup> Collaborative Center of Control Science, Department of Electrical Engineering, The Ohio State University, Columbus, OH 43210, U.S.A.,

yuanx@ee.eng.ohio-state.edu

<sup>2</sup> Collaborative Center of Control Science, Department of Electrical Engineering, The Ohio State University, Columbus, OH 43210, U.S.A. [onderefe@ieee.org](mailto:onderefe@ieee.org)

<sup>3</sup> Department of Electrical and Electronics Engineering, Bilkent University, Bilkent, Ankara, TR-06800, Turkey; on leave from The Ohio State University, [ozbay@ee.eng.ohio-state.edu](mailto:ozbay@ee.eng.ohio-state.edu)

**Summary.** Design and implementation of flow control problems pose challenging difficulties as the flow dynamics are governed by coupled nonlinear equations. Recent research outcomes stipulate that the problem can be studied either from a reduced order modeling point of view or from a transfer function point of view. The latter identifies the physics of the problem on the basis of separate components such as scattering, acoustics, shear layer etc. This paper uses the transfer function representation and demonstrates a good match between the real-time observations and a well-tuned transfer function can be obtained. Utilizing the devised model, an  $H_\infty$  controller based on Toker-Özbay formula is presented. The simulation results illustrate that the effect of the noise can be eliminated significantly by appropriately exciting the flow dynamics.

## 1 Introduction

Aerodynamic flow control is a core issue aiming to reduce skin friction thereby increasing the maneuverability of aerial vehicles and reducing the fuel expenditure. The research towards this goal is in its infancy, however, some major problems have been identified. These particularly include the development of a dynamic model for a given flow geometry, and describing the best control scheme in some sense of optimality. In this paper we discuss cavity flow problem.

One of the two branches of research towards the model development for cavity flow stipulate the use of proper orthogonal decomposition techniques to remedy the problem of infinite dimensionality, [1],[2]. These procedures yield a set of ordinary differential equations, which are autonomous. The underlying idea is to extract the most dominant features (modes) containing the essential

part of the flow energy. Although the modeling issue has well been addressed, the control design is still dependent upon models that explicitly include the control input. The other viewpoint exploits the strength of representing the physical properties by dynamical models in transfer function forms, [3],[4],[5]. Cited studies demonstrate that the shear layer, scattering, cavity acoustics and receptivity can be represented dynamically as transfer functions. Due to the reflections from the upstream wall of the cavity, after some propagation delay time, the reflections interact with the oncoming flow and a delay-based coupled dynamics arise. It must be noted that the devised form of the transfer function matches the frequency content of the data obtained from Navier-Stokes equations.

In this paper, we optimize the parameters of the model developed in [3],[4],[5] to match the magnitude and frequencies of the resonant peaks and use this model to synthesize an  $H_\infty$  controller.

It is a well known fact that  $H_\infty$  controller design scheme is particularly well suited if the model involves uncertainties. This study demonstrates that an optimal controller can be determined by utilizing the framework presented in [6].

The paper is organized as follows: Section 2 introduces the transfer function based model of the cavity flows with its sub-components. The third section is devoted to the parameter tuning issues. The frequency response match is presented in that section. Following this, the methodology to design an  $H_\infty$  controller is discussed together with the simulation results. Concluding remarks are made in the last section.

## 2 Delay-Based Models of Cavity Flow

The process shown in Figure 1 is for cavity flows, which constitute the simplest geometry for studying aerodynamic flow control problems. Basically, this representation captures major dynamic phenomena inside the flow field. For the shear layer, we have,

$$G(s) = G_0(s)e^{-s\tau_s}, \quad (1)$$

where  $\tau_s = L/(\kappa U)$  (with  $L$  being the length of the cavity,  $U$  being the freestream velocity and  $\kappa$  is a known constant). In (1),  $G_0(s) = \frac{\omega_0^2}{s^2 + 2\zeta\omega_0 s + \omega_0^2}$  with  $\omega_0$  and  $\zeta$  are the natural frequency and damping ratio, respectively.

The acoustics term is given as

$$A(s) = \frac{e^{-s\tau_a}}{1 - re^{-2s\tau_a}}, \quad (2)$$

where

$$r(s) = \frac{r}{1 + s/\omega_r}, \quad (3)$$

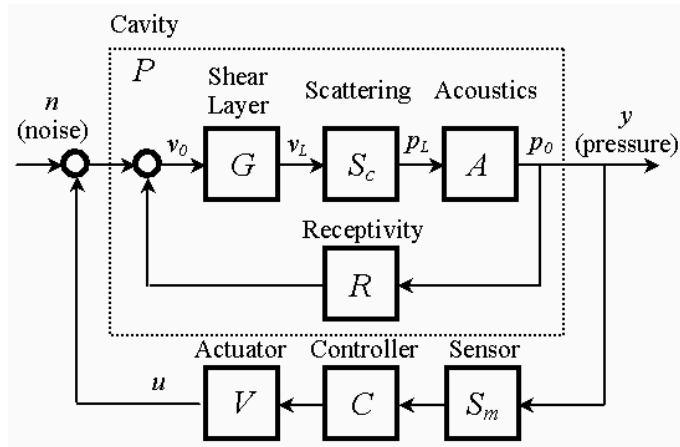


Fig. 1. Block representation of the cavity flow and the control loop[3],[4]

is the attenuation factor of the reflection process. Denoting the speed of sound by  $a$ , the time delay representing the acoustic lag between the trailing edge and the leading edge is given as  $\tau_a = L/a$ . Here, the Mach number can be calculated as  $M = U/a$ . Furthermore, the numerical values of  $R$  (receptivity),  $S_c$  (scattering),  $V$  (actuator) and  $S_m$  (sensor) are assumed to be available in [4] and denote them by  $K_R$ ,  $K_S$ ,  $K_v$  and  $K_m$  respectively. In the view of these, the cavity transfer function  $P$  can be formed as given below:

$$P(s) = \frac{AS_cG}{1 - RAS_cG}. \quad (4)$$

Although the system is a linear one, at some Mach numbers unstable limit cycling appears. The focus of this paper is to study how a robust controller can be devised under dynamic uncertainties.

The goal of the controller is to reduce the peak value of  $|P(j\omega)S(j\omega)|$ , where  $S(j\omega)$  is the sensitivity function, so that the effect of the noise at the output is reduced. An example of achieving such a goal can be found in [4], in which the controller is composed of a filter followed by a gain and a time delay. In the next section, we outline the effect of each parameter on the frequency response characteristics.

### 3 Parameter Tuning for the Flow Dynamics

Our studies have demonstrated that the flow dynamics developed by Rowley *et al.*, [4], [5] exhibit certain degrees of flexibility to match the frequency response obtained from the real-time data with that of the input-output model. In

order to analyze this, we have performed several tests to see which parameter is responsible for introducing what sort of modification into the frequency content. Following is a list summarizing our conclusions in this respect:

As  $\omega_0$  increases, the dominant peak moves towards higher frequencies. The frequency domain picture is stretched to the right.

As  $\zeta$  increases, the values of the peaks get lowered, and the frequency content becomes more flattened.

An increase in  $K_S$  lifts up the entire frequency domain picture while magnifying the peak values slightly.

If  $r$  is increased, more peaks appear particularly in the higher frequencies.

As  $\tau_s$  increases, the frequency response acquires more fluctuations (peaks) in the low frequencies. Further increments lead to more wavy low frequency behavior.

Change in  $\tau_a$  causes small translations with some tiny changes in the peak magnitudes.

As  $K_R$  increases, the peak magnitudes get larger.

Apparently, the above information constitutes a knowledge base for us, and lets us know how to tune the parameters given some real-time data.

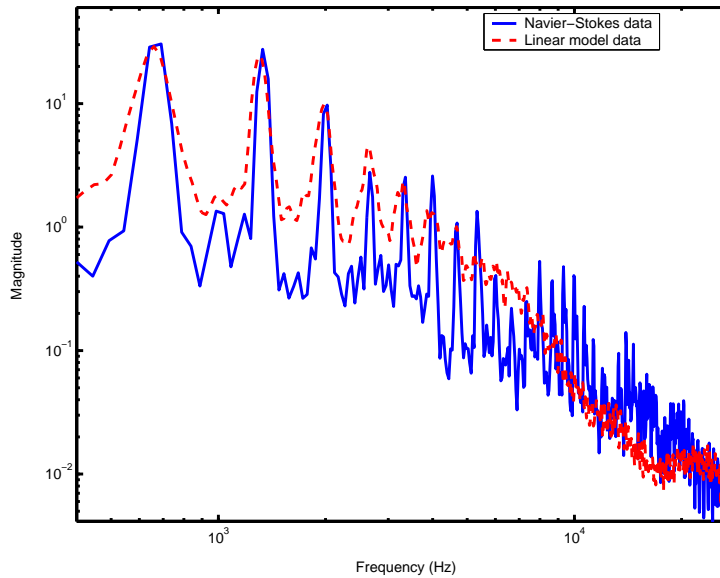


**Fig. 2.** Power spectral density comparison of pressure data obtained from full order Navier-Stokes simulation and data from the model in (4)

In this paper, we use trial and error method to match the frequency content and the result of the model match is illustrated by Figure 2, from which we can

see that the power spectral density of the simulation output of the linear model matches that of the simulation outputs based on Navier-Stokes equations very well. The data for the linear system are given in Table 1, on which the robust controller design is based.

**Table 1.** Parameters of the Linear Model

Parameter	Value
$\omega_0$	200 rad/sec
$\zeta$	0.95
$\tau_s$	0.0195 sec
$\tau_a$	0.001 sec
$r$	0.1
$\omega_r$	100 rad/sec
$K_R$	0.408
$K_S$	1.65
$K_v$	1
$K_m$	1

## 4 Robust Controller Design

Inserting the transfer functions of the shear layer and the acoustics into the plant transfer function, we get

$$\begin{aligned}
 P(s) &= \frac{\frac{\omega_0^2}{s^2+2\zeta\omega_0s+\omega_0^2} e^{-s\tau_s} K_s \frac{e^{-s\tau_a}}{1-re^{-2s\tau_a}}}{1 - K_R \frac{\omega_0^2}{s^2+2\zeta\omega_0s+\omega_0^2} e^{-s\tau_s} K_s \frac{e^{-s\tau_a}}{1-re^{-2s\tau_a}}}, \\
 &= \frac{K_S \omega_0^2 e^{-s(\tau_s+\tau_a)}}{(s^2 + 2\zeta\omega_0s + \omega_0^2)(1 - re^{-2s\tau_a}) - K_R K_S \omega_0^2 e^{-s(\tau_s+\tau_a)}}, \\
 &= \frac{K_S \omega_0^2 e^{-s(\tau_s+\tau_a)}}{(s^2 + 2\zeta\omega_0s + \omega_0^2) - r(s^2 + 2\zeta\omega_0s + \omega_0^2)e^{-2s\tau_a} - K_R K_S \omega_0^2 e^{-s(\tau_s+\tau_a)}}.
 \end{aligned} \tag{5}$$

Let us factorize  $P(s)$  into the form  $P(s) = N_{o1}(s)N_{o2}(s)M_n(s)$ , where

$$N_{o2}(s) = K_S G_0(s) = \frac{K_S}{1 + 2\zeta s/\omega_0 + s^2/\omega_0^2}, \tag{6}$$

$$M_n(s) = e^{-h_1 s}, \quad \text{where } h_1 = \tau_s + \tau_a, \tag{7}$$

$$N_{o1}(s) = (1 - K_R N_{o2}(s)M_n(s) - r(s)M_2(s))^{-1}, \tag{8}$$

where  $M_2(s) = e^{-2\tau_a s}$ . Plant is stable for the numerical values determined in this case. For different numerical values it is possible to have an unstable plant,

then finitely many unstable modes may appear from the roots of  $1/N_{o1}(s) = 0$ . This situation can be handled in our approach as well. At this stage, we propose to use Toker-Özbay formula (see [6]) to design the controller. The optimal robust performance is defined by

$$\gamma_{opt} := \inf_{C \in \Omega} \left\| \begin{pmatrix} W_1 S \\ W_2 T \end{pmatrix} \right\|_{\infty}, \quad (9)$$

where  $\Omega$  is the set of all compensators stabilizing  $P$ . It is known that  $S = (1 + PC)^{-1}$  and  $T = 1 - S$  are the sensitivity and complementary sensitivity functions and  $W_1$  and  $W_2$  are the performance and stability weighting functions. Since the goal of the controller is to reduce the peak value of  $|P(j\omega)S(j\omega)|$ , we choose the performance weighting function  $W_1(s)$  as given in (11), such that the oscillation magnitude at the dominating modes is suppressed. To take care of the uncertainties in the high frequency, we set the complementary sensitivity weighting function  $W_2(s)$  as given by (13). In Figure 3, Bode plots of these weighting functions and the plant are depicted.

$$W_{1o}(s) = k_1 \frac{(1 + s/\omega_{1n})}{(1 + s/\omega_{1d})}, \quad (10)$$

$$W_1(s) = W_{1o}(s)(1 - r(s)M_2(s))N_{o1}(s), \quad (11)$$

$$W_{2o}(s) = \epsilon_2 s(1 + s/\omega_{1n}), \quad (12)$$

$$W_2(s) = W_{2o}(s)(1 - r(s)M_2(s)). \quad (13)$$

Define the following functions

$$P_2 = N_{o2}M_n, \quad (14)$$

$$S_2 = (1 + P_2 C_2)^{-1}, \quad (15)$$

$$T_2 = 1 - S_2. \quad (16)$$

By inverting the outer part of the plant, we see that the  $H_{\infty}$  controller has to be in the form  $C(s) = C_2(s)(1 - r(s)M_2(s)) + K_R$ , where  $C_2$  is designed for

$$\gamma = \inf_{C_2 \text{ stabilizes } P_2} \left\| \begin{pmatrix} W_{1o} S_2 \\ W_{2o} T_2 \end{pmatrix} \right\|_{\infty} \quad (17)$$

By definition, it can be seen that the performance specifications of both systems are equivalent, i.e.,

$$|W_1(j\omega)S(j\omega)| = |W_{1o}(j\omega)S_2(j\omega)|, \quad (18)$$

For the robustness of the system, it can be shown that if

$$\left| \frac{\Delta_{P_2}}{P_2} \right| < \left| \gamma^{-1} W_{2o} \right|, \quad (19)$$

$$\left| \Delta_{K_R} \right| < \left| \gamma^{-1} \frac{W_{1o} N_{o1} (1 - r M_2)^2}{N_{o2}} \right|. \quad (20)$$

then the system associated with plant  $P$  and controller  $C$  is robustly stable, where  $\Delta_{P_2}$  denotes the uncertainty of the plant  $P_2$  and  $\Delta_{K_R}$  is the uncertainty of the variable  $K_R$ . The problem is significantly simplified such that  $C_2$  can be computed explicitly by hand calculations. The optimal controller  $C_2$  for  $P_2$  is in the form

$$C_2(s) = \left( \frac{\gamma}{\gamma_{min}} - \frac{\gamma_{min}}{\gamma} \right) \frac{N_{o2}^{-1}(s)}{(1 + as + bs^2)} \left( \frac{1}{1 + H(s)} \right), \quad (21)$$

To compute the optimal performance level  $\gamma$ , define

$$\gamma_{min} := k_1 \frac{\omega_{1d}}{\omega_{1n}}, \quad (22)$$

$$\gamma_{max} := k_1, \quad (23)$$

and

$$x = \sqrt{\frac{k_1^2 - \gamma^2}{\gamma^2 - \gamma_{min}^2}}, \quad (24)$$

$$b = \frac{\epsilon_2 \sqrt{1 - (\gamma_{min}/\gamma)^2}}{k_1 \omega_{1d}}, \quad (25)$$

$$a = \sqrt{2b + \epsilon_2^2 (k_1^{-2} - \gamma^{-2})}. \quad (26)$$

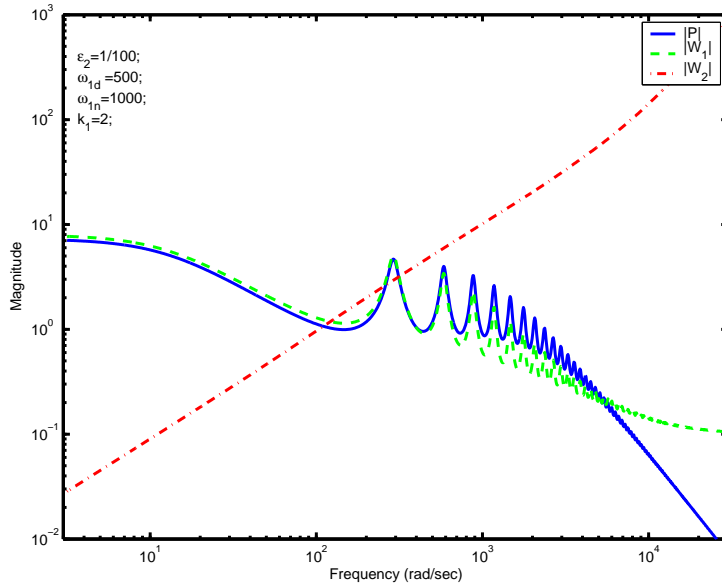


Fig. 3. Weighting functions

Taking the largest value of  $\gamma$  satisfying the below equality (27) in the allowable range:  $\gamma_{max} > \gamma > \gamma_{min}$  will give us the optimal  $\gamma$  needed in the optimal controller formula (21). For the current problem, we obtain  $\gamma = 1.9484$ .

$$\pi = h_1\omega_{1d}x + \tan^{-1}x + \tan^{-1}\frac{\omega_{1d}x}{\omega_{1n}} + \tan^{-1}\frac{a\omega_{1d}x}{1 - b\omega_{1d}^2x^2}. \quad (27)$$

To implement the controller in real-time,  $H(s)$  is expanded as a finite impulse response (FIR) filter and an exponential decay term, i.e.  $H(s) = H_{FIR}(s) + H_{IIR}(s)$ , which are described in (28) and (29). The magnitude of  $H(s)$  and its constituents are shown in Figure 7.

$$H_{FIR}(s) = \frac{(\omega_{1d} + \omega_{1n})s + \omega_{1n}\omega_{1d} - \omega_x^2 + \frac{\gamma}{\gamma_{min}}\omega_{1d}^2(1+x^2)(d_1s + d_0)e^{-h_1s}}{s^2 + \omega_x^2}, \quad (28)$$

$$H_{IIR}(s) = \frac{\gamma}{\gamma_{min}} \left( \frac{\omega_{1d}^2(1+x^2)(c_1s + c_0) - 1}{1 + as + bs^2} \right) e^{-h_1s}, \quad (29)$$

in which  $c_0$ ,  $c_1$ ,  $d_0$ ,  $d_1$  and  $\omega_x$  are defined as below:

$$c_0 = \frac{(b(1 - b\omega_x^2) - a^2)}{a}d_1, \quad (30)$$

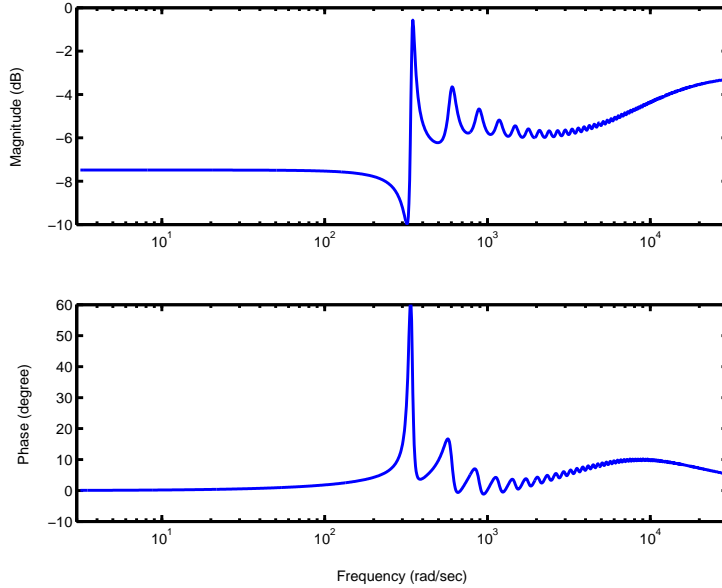


**Fig. 4.** Bode plot of the optimal controller



$$c_1 = -bd_1, \tag{31}$$

$$d_0 = d_1 \frac{(b\omega_x^2 - 1)}{a}, \tag{32}$$

$$d_1 = \frac{-a}{\omega_x^2 a^2 + (1 - b\omega_x^2)^2}, \tag{33}$$

$$\omega_x = \omega_{1d}x. \tag{34}$$

It has been demonstrated that the impulse response of  $H_{FIR}(s)$  is restricted to the time interval  $[0, h_1]$ , which is shown in Figure 6. Hence,  $H_{FIR}(s)$  can be realized as a FIR filter of duration  $h_1$ . The discrete-time realization of  $H_{FIR}(s)$  requires only  $h_1/T_s$  states, where  $T_s$  is the sampling period. Theoretically, the infinite dimensional controller can be implemented through a finite impulse response (FIR) filter approximation.

In Figure 4, we demonstrate the Bode plot of the controller, which has been discussed above. Figure 8 illustrates the Bode plot of the closed loop control system compared to the open loop plant. As the figure suggests, the controller modifies the frequency content of the open loop system significantly at the dominating modes. The resonant peaks in the frequency response of the open loop system are suppressed and the improvement is obvious. Figure 9 shows the time domain simulation result of the the closed loop system.

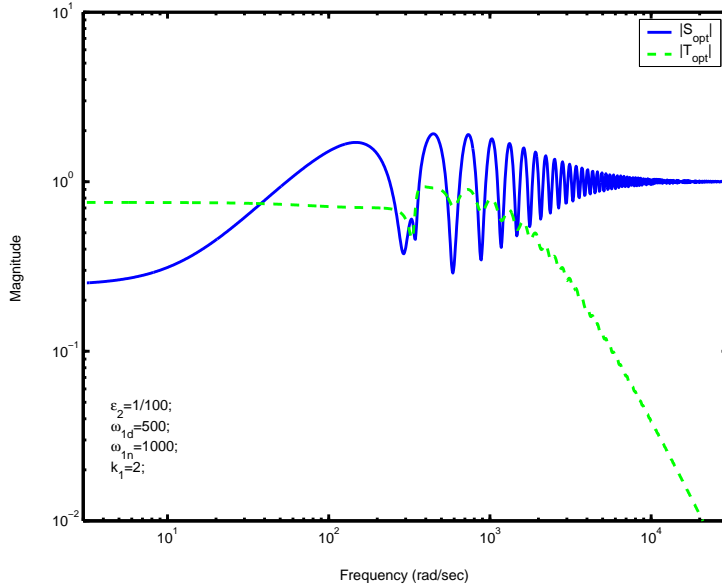


Fig. 5. Optimal  $S$  and  $T$

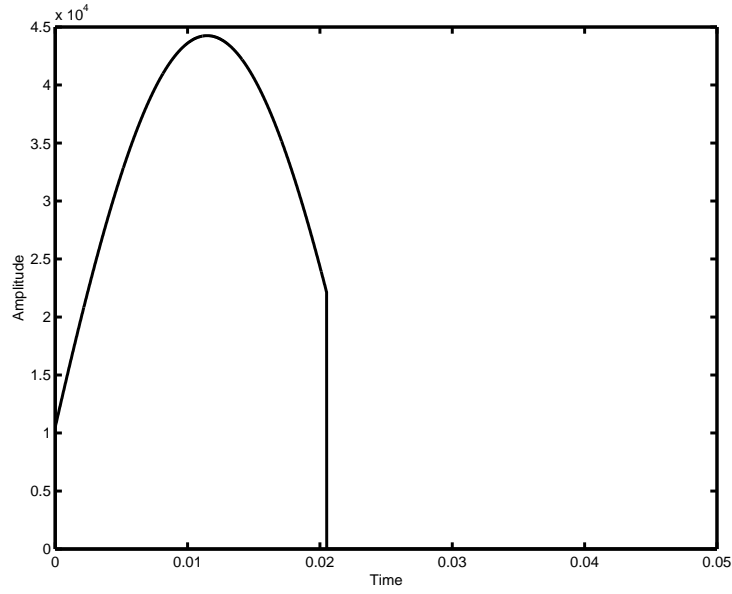


Fig. 6. Impulse response of  $H_{FIR}(s)$

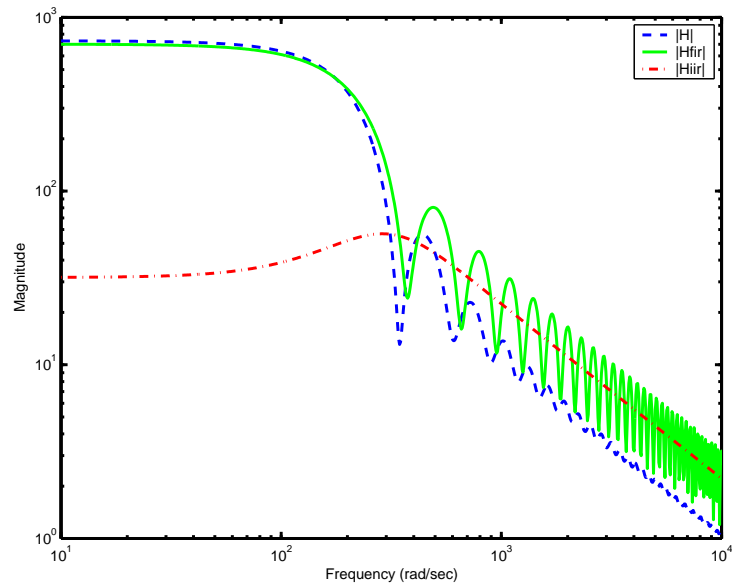
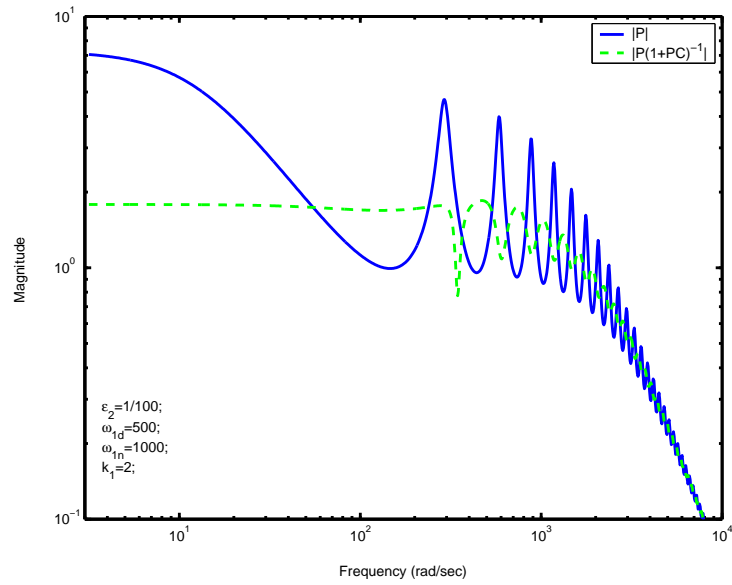
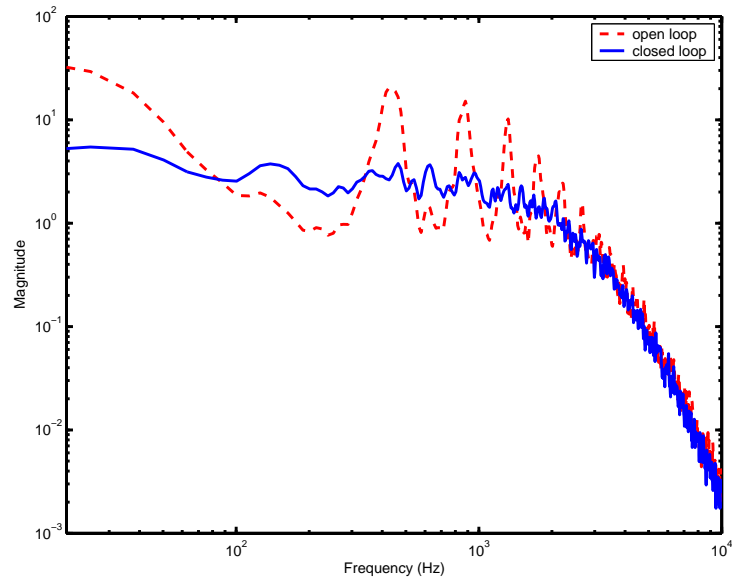


Fig. 7. Magnitude of  $H(s)$ ,  $H_{FIR}(s)$  and  $H_{IIR}(s)$



**Fig. 8.** Bode plot of the closed loop system compared with that of the open loop system



**Fig. 9.** Power spectral density of output of time domain simulation

## 5 Conclusions

In this study, we focus on the transfer function based models of cavity flows. Due to the delays inherited from the physics of the problem, the problem is an infinite dimensional one. We demonstrate that a previously studied form of delay-based flow model can be tuned so as to capture the resonant peaks appearing in the frequency response. We present how a  $H_\infty$  based controller can be devised for such a Single-Input-Single-Output system. The observed results demonstrate that the controller performs well under the presence of uncertainties. The undesired resonant peaks of the open loop system have been suppressed fairly well.

## 6 Acknowledgments

This work was supported in part by AFRL/AFOSR under the agreement no. F33615-01-2-3154, and by the National Science Foundation.

The authors would like to thank Prof. M. Samimy, Dr. J.H. Myatt, Dr. J. DeBonis, Dr. M. Debiasi, and E. Caraballo for fruitful discussions in devising the presented work.

## References

1. Ravindran SS (2000). A Reduced Order Approach for Optimal Control of Fluids Using Proper Orthogonal Decomposition. *International Journal for Numerical Methods in Fluids*, 34:425-488.
2. Atwell JA, King BB (2001). Proper Orthogonal Decomposition for Reduced Basis Feedback Controllers for Parabolic Equations. *Mathematical and Computer Modelling of Dynamical Systems*, 33:1-19.
3. Williams DR, Rowley CW, Colonius T, Murray RM, MacMartin DG, Fabris D, Albertson J (2002). Model Based Control of Cavity Oscillations Part I: Experiments. 40th Aerospace Sciences Meeting (AIAA 2002-0971), Reno, NV.
4. Rowley CW, Williams DR, Colonius T, Murray RM, MacMartin DG, Fabris D (2002). Model Based Control of Cavity Oscillations Part II: System Identification and Analysis. 40th Aerospace Sciences Meeting (AIAA 2002-0972), Reno, NV.
5. Rowley CW, Colonius T, Murray RM (2001). Dynamical Models for Control of Cavity Oscillations. 7th AIAA/CEAS Aeroacoustics Conf. (AIAA 2001-2126), May 28-30, Maastricht, The Netherlands.
6. Toker O, Özbay H (1995).  $H_\infty$  Optimal and Suboptimal Controllers for Infinite Dimensional SISO Plants. *IEEE Transactions on Automatic Control*, 40:751-755.